A new drug-sensing paradigm based on ion-current rectification in a conically shaped nanopore

JiaHai Wang[1] *& Charles R Martin*[1†]

[†]*Author for correspondence*
[1]*University of Florida, Department of Chemistry & Center for Research at the Bio/Nano Interface, Gainesville, FL 32605, USA*
Email: crmartin@chem.ufl.edu

Aims: To utilize the ion-current rectification phenomenon observed for conically shaped nanopores as the basis for designing sensors for drug molecules that adsorb to the walls of the nanopore. **Methods:** The conically shaped nanopore was prepared by the well-known track-etch method in a polyimide (Kapton) membrane. The ion current flowing through the nanopore was measured as a function of applied transmembrane potential in the presence of the analyte drug molecule, Hoechst 33258. **Results:** The pore walls in the Kapton membrane are hydrophobic yet have fixed carboxylate groups that give the walls a net negative charge. This fixed anionic surface charge causes the nanopore to rectify the ion current flowing through it. The analyte drug molecule, Hoechst 33258, is cationic yet also hydrophobic. When the membrane is exposed to this molecule, it adsorbs to the pore walls and neutralizes the anionic surface charge, thus lowering the extent of ion-current rectification. The change in rectification is proportional to the concentration of the drug. **Conclusions:** This nanopore sensor is selective for hydrophobic cations relative to anions, neutral molecules and less hydrophobic cations. Future work will explore ways of augmenting this hydrophobic effect-based selectivity so that more highly selective sensors can be obtained.

There is increasing interest in using nanopores in synthetic [1–21] or biological [22–39] membranes as biosensors. Perhaps the most popular nanopore-based sensing paradigm is the well-known resistive-pulse, or stochastic-sensing, method which entails counting individual analyte molecules as they are driven through the nanopore sensor element [1–39]. Prototype sensors for analyte species as diverse as proteins, DNA and small molecules have been described. While we too are exploring resistive-pulse sensors [6,7,40], we have also been investigating other sensing paradigms based on artificial nanopores [4]. One such paradigm makes use of the well-known ion-current rectification phenomenon displayed by conically shaped nanopores [41–48].

The sensor element in this case is a single conically shaped nanopore in a polyimide (Kapton) membrane [7,49]. A conically shaped nanopore has two openings – the small diameter (tip) opening at one face of the membrane and the large diameter (base) opening at the opposite face. The sensing paradigm entails placing electrolyte solutions on either side of the membrane and using electrodes in each solution to scan the applied transmembrane potential and measure the resulting ion current flowing through the nanopore (Figure 1). As has been discussed in detail by us [41,42] and others [43–49], conically shaped nanopores with excess surface charge on the pore walls, and sufficiently small tip openings, show nonlinear current voltage curves; in other words, such pores are ion-current rectifiers. Because the polyimide nanopores used here have excess anionic surface charge, rectification is observed at positive applied transmembrane potential [47].

We have found, however, that when the nanopore is exposed to a very hydrophobic, yet cationic, drug molecule (Hoechst 33258; Figure 2), adsorption of this molecule on the pore walls neutralizes the excess negative surface charge. As a result the nanopore does not rectify as strongly, and the magnitude of the decrease in rectification scales with the concentration of the drug molecule. Ultimately, at high concentrations of the drug, the sign of the excess surface charge switches from net negative to net positive, and the nanopore rectifies at negative applied transmembrane potential [41]. We describe this new nanopore-based sensing paradigm here.

Materials & methods

Membranes & chemicals

Polyimide (Kapton; Figure 2) membranes (diameter = 3 cm, thickness = 12 µm) that had been irradiated with a heavy ion of 2.2 GeV kinetic energy to create a single damage track through the membrane were obtained from GSI, Darmstadt, Germany [7,49]. We refer to these as-received membranes as the 'tracked' membranes.

Keywords: conical nanopores, drug sensors, Hoechst 33258, ion-current rectification

future medicine part of fsg

Figure 1. I–V curves for a conical nanopore sensor (tip diameter = 67 nm, base diameter 1.4 µm) in the presence of various concentrations of Hoechst 33258.

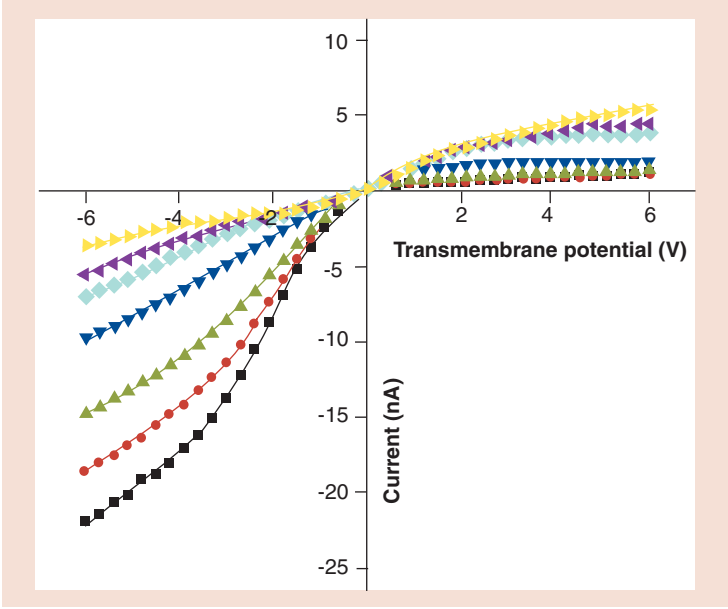

0 nM (black squares, lower most curve), 1.25 µM (red circles), 2.5 µM (green triangles), 5 µM (blue triangles), 10 µM (cyan diamonds), 15 µM (magenta triangles), 25 µM (yellow triangles, upper most curve).

Hoechst 33258, methyl viologen dichloride hydrate, benzyl viologen and sodium hypochlorite (13% active chloride) were purchased from Sigma-Aldrich and used as received. *Bis-tris* propane, used to prepare the buffer solutions, was also obtained from Aldrich. All other chemicals were used as received. Purified water was prepared by passing house-distilled water through a Millipore Milli-Q water purification system.

Etching the conical nanopore in the tracked membrane

We recently described a two-step etching procedure for reproducibly preparing conically shaped nanopores in tracked poly(ethylene terphthalate membranes) [50]. A variant of that method was used to etch the conical nanopores in the tracked Kapton membranes used for these studies. The tracked Kapton membrane was first irradiated under UV light (320 nm) for 15 h, and then mounted in a two-compartment cell [50] such that electrolyte solution could be placed on either side of the tracked membrane.

The first etch step, developed by Apel *et al.* [49], entailed placing a solution that etched the damage track (13% NaOCl, pH = 12.6) on one side of the membrane and a solution that neutralizes the etchant (2M KI, the 'stop' solution) on the other side [7]. The temperature during etch was 50°C. Each half cell contained a Pt wire (diameter = 0.2 cm, length ~7.6 cm), and a Keithley 6487 picoammeter/voltage-source (Keithley Instruments, Cleveland, OH, USA) was used to apply a transmembrane potential of 1 V during etching and measure the resulting ionic current flowing through the nascent nanopore. The current was initially zero but increased suddenly when the etch solution broke through to the stop solution. This first etch step was terminated when the current reached 0.1 nA. At this point, stop solution was placed in both half cells to quench the etch.

As per our prior work [7], the diameter of the base opening after the first etch step was determined by obtaining scanning electron micrographs of the base side of multitrack Kapton membranes etched in the analogous way. Multitrack membranes (1×10^6 tracks cm^{-2}, also from GSI) were used because it is difficult to find the base openings by electron microscopy in etched single-track membranes. These studies yielded an etch rate of 8.3 nm/min, similar to the value of 7.0 nm/min, obtained by Siwy *et al.* [51]. Our studies with PET membranes showed that by varying the etch time (or final etch current) or the transmembrane voltage applied during etching, the base diameter can be reproducibly controlled during this first etch step [50,52]. We found, however, that it is difficult to reproducibly control the tip diameter. This led us to subject the membrane to a second etch step, which allows us to control and fine-tune the tip diameter [50].

The second etch step entailed placing the NaOCl etch solution on both sides of the membrane. A transmembrane potential of 200 mV was applied, and again the transmembrane current was monitored during the etch. This etch was stopped at a prescribed value of the transmembrane current [50]. We found that this allows for excellent reproducibility in both tip and base diameter [50]. The base and tip diameters after the second etch were measured using the electrochemical method described in detail previously [50]. Membranes with two different base and tip diameters were used for these studies. The first had base diameter of 1.4 µm and tip diameter of 67 nm. The second had base diameter of 2.0 µm and tip diameter of 48 nm.

Sensing the analyte molecules

The membrane containing the conically shaped nanopore was mounted in the two-compartment cell [50], and a solution containing the desired

Figure 2. Analyte molecules studied with the nanopore sensor.

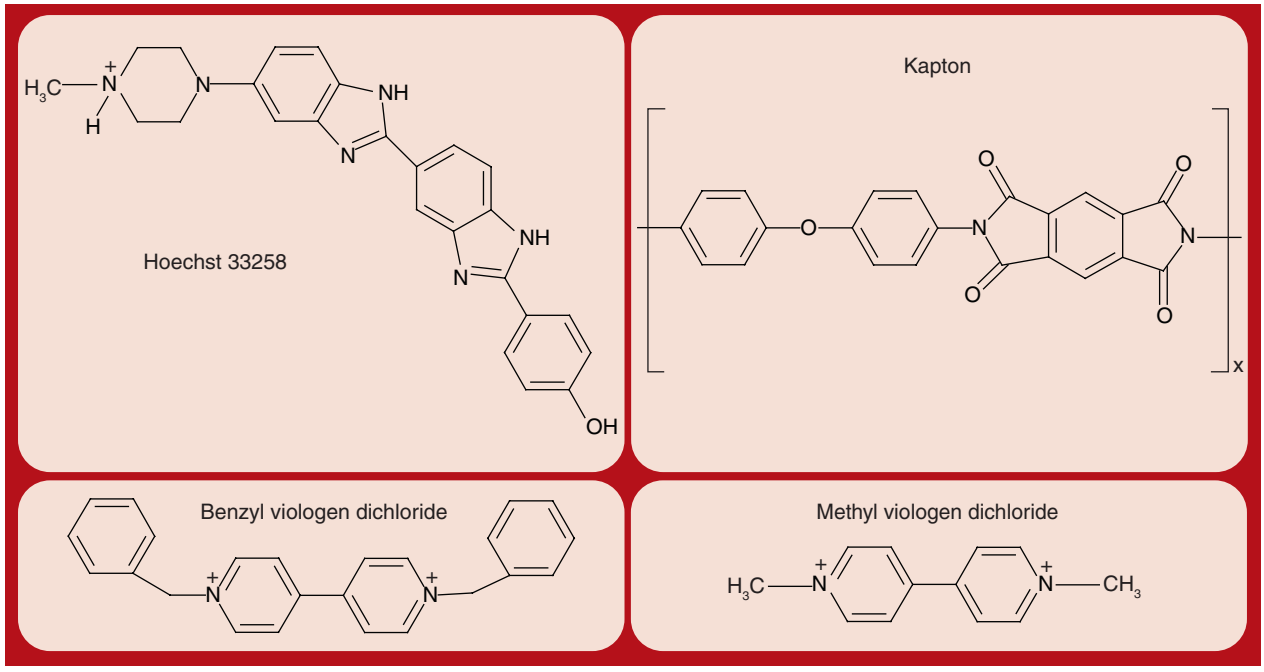

analyte molecule (Figure 2) was placed on the side of the membrane containing the tip opening. (The response time appeared to be longer in preliminary studies of base-side exposure.) This solution was prepared in 10 mM *bis-tris* propane (pH = 7.0) that was also 3 mM in $MgCl_2$, and the same buffer solution, devoid of the analyte, was placed on the opposite side on the membrane. A Ag/AgCl electrode was placed into each solution, and the Keithley 6487 was used to obtain a current–voltage (I–V) curve associated with ion transport through the nanopore. The working Ag/AgCl electrode was in the half-cell facing the base opening, and the potential of this electrode was controlled relative to the counter Ag/AgCl electrode in the opposite solution. The I–V curve was obtained by stepping the potential in 300 mV steps through the desired potential range. The sign convention used here is the same as that used in our prior studies – negative transmembrane potentials mean that the cathode is in the solution facing the base opening and the anode is in the solution facing the tip opening [41].

Results & discussion

Ion-current rectification by conical nanopores

Figure 1 shows I–V curves for a conical nanopore in a Kapton membrane with and without the analyte drug molecule Hoechst 33258. In the absence of this drug, the I–V curve is nonlinear, indicating that the nanopore strongly rectifies the ion current flowing through it [41,43–48]. While there is currently some disagreement in the literature as to the precise mechanism by which conical nanopores rectify the ion current [41,43–48], all extant theories agree on the following: rectification requires that excess charge be present on the pore walls and that the diameter of the tip opening be comparable to the thickness of the electrical double layer extending from the pore wall.

The ion-current rectification phenomenon can be described qualitatively by defining 'on' and 'off' states for the nanopore rectifier [41]. In agreement with previous results for conically shaped Kapton nanopores, in the absence of Hoechst 33258, the on state occurs at negative potentials and the off state at positive potentials (Figure 1) [41]. This indicates that rectification is caused by fixed anionic (carboxylate) groups on the pore wall [47,51]. The extent of rectification can be quantified by the rectification ratio [41,42], defined here as the current at -6.0 V divided by the current at +6.0 V (Table 1).

Effect of Hoechst 33258 on recatification

The key experimental observations for these studies are:

- As Hoechst 33258 is added, the extent of rectification decreases (Figure 1)

Table 1. Rectification ratio as a function of drug concentration.

Concentration (µM)	Rectification ratio
0	19.6
2.5	10.8
5	4.9
10	1.9
15	1.2
25	0.67

- The extent of rectification scales inversely with the concentration of Hoechst 33258 (Table 1)
- Ultimately, at high drug concentrations, the rectification is reversed (Figure 1, Table 1)

This reversal in rectification is signaled by the fact that at high drug concentrations the on state is at positive potentials and the off state is at negative potentials. Rectification with this polarity causes the rectification ratio to be less than unity (Table 1). We have demonstrated that rectification with this polarity requires excess positive charge on the pore walls [41].

Figure 3. Response of the sensor to methyl and benzyl viologen.

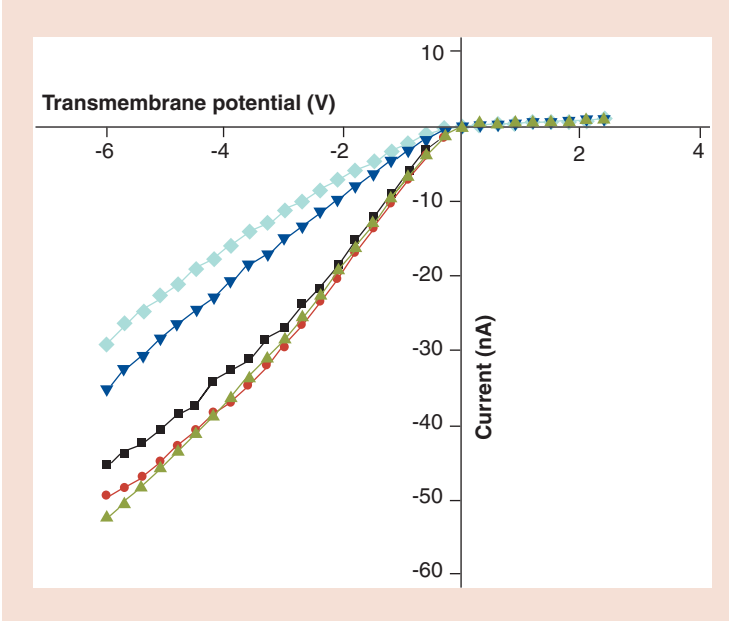

I–V curves for a conical nanopore sensor (tip diameter = 48 nm, base diameter 2.0 µm) in the presence of 2.3 mM methyl viologen (green triangles, lower most curve), 1 mM methyl viologen (circles), buffer only (squares), 1 mM benzyl viologen (triangles) and 2.3 mM benzyl viologen (diamonds, upper most curve).

At a pH of 7.0, Hoechst 33258 is cationic with a net charge of +1 [53], owing to protonation of the methyl-substituted piperdine-like N. In addition, this drug is quite hydrophobic, as is Kapton polyimide, with a dielectric constant of 3.4. We have shown that such hydrophobic cationic drug molecules can adsorb to hydrophobic surfaces and impart positive charge to the surface [54]. These prior studies provide a simple explanation for the results in Figure 1. Exposure of the hydrophobic Kapton membrane to the cationic and hydrophobic Hoechst 33258 causes this molecule to adsorb to the pore wall, thus neutralizing the surface-carboxylate sites, and this neutralization of the negative surface charge causes the observed decrease in ion current rectification (Table 1). The reversal of polarity at high drug concentrations (Figure 1), and concomitant less-than-unity rectification ratios (Table 1), indicate that ultimately the quantity of adsorbed cationic charge due to the drug exceeds the quantity of fixed negative charge due to the surface carboxylates.

This reversal in the sign of the surface charge illustrates an important chemical point. At low drug concentrations, where the net surface charge on the pore wall is negative, there is no question that part of the interaction between the drug and the surface is electrostatic – the surface needs a charge balancing cation and it chooses the hydrophobic drug over the inorganic cations present in the solution. However, this electrostatic component is augmented by the hydrophobic component, as indicated by the fact that when the net surface charge becomes positive at high drug concentrations, the drug continues to adsorb. For example, the less-than-unity rectification ratio for 25 µM of drug (Table 1) indicates that the surface has net positive charge when the membrane is exposed to this drug concentration.

Effect of benzyl & methyl viologen on rectification

To explore the surface chemical interactions further, we obtained analogous data for two other relatively hydrophobic cationic molecules – methyl and benzyl viologen (Figure 2). Current voltage curves for a conical nanopore sensor before and after exposure to these molecules are shown in Figure 3. The black curve was obtained in the absence of the viologens, and, as before, shows the strong surface carboxylate-induced rectification phenomenon. In analogy to Hoechst 33258, the more hydrophobic benzyl viologen engenders a concentration-dependent

Table 2. Current at -6V as a function of drug concentration.

Concentration (μM)	Current (nA)
0	-21.9
2.5	-14.8
5	-9.8
10	-7.0
15	-5.4
25	-3.6
500	-4.6
1000	-6.0
1500	-6.1

decrease in the extent of rectification. However, the concentrations required to produce a measurable change are approximately three orders of magnitude higher than the concentration needed for Hoechst 33258. This clearly shows that benzyl viologen adsorbs much more weakly to the Kapton surface than Hoechst 33258.

This observation helps us understand the relative contributions of hydrophobicity versus molecular charge to the interaction of the adsorbing molecule with the Kapton surface. Recall first that benzyl viologen is a divalent cation, whereas Hoechst 33258 is monovalent. If the interaction between the adsorbing molecule and the Kapton surface was dominated by electrostatics, then benzyl viologen would adsorb more strongly, and this is not what is observed experimentally. Hence, it is clear that the hydrophobic effect is the dominant force that causes adsorption to the Kapton surface. This is in agreement with our early observation that cationic Hoechst 33258 continues to adsorb even after the Kapton surface has net positive charge. This conclusion is also in agreement with our prior work which showed that hydrophobic, yet cationic, drugs adsorb to neutral hydrophobic surfaces [54].

The dominance of the hydrophobic effect is also strongly reinforced by the methyl viologen data in Figure 3. Methyl viologen retains the 2+ charge of benzyl viologen, but because it lacks the two benzene rings, it is much less hydrophobic. As a result, no evidence for methyl viologen adsorption is observed in Figure 3. A slight increase in current, relative to the I–V curve obtained in the absence of methyl viologen, is observed because at the mM and higher concentrations used, the divalent methyl viologen makes a measurable contribution to the bulk conductivity of the electrolyte.

Langmuir analysis of the Hoechst 33258 adsorption data

We can write the following general equation for Langmuir adsorption of a molecule to a surface [54]:

$$\Theta = KC/(1 + KC) \quad (1)$$

where Θ is the fractional coverage of the molecule on the surface, K is the binding constant with units of $lmol^{-1}$ and C is the concentration of the drug in the contacting solution phase. Θ is also given by:

$$\Theta = mole_{D,i}/mole_{D,max} \quad (2)$$

where $mole_{D,i}$ is the number of moles of drug on the surface when the membrane is exposed to some concentration of drug, i, and $mole_{D,max}$ is the maximum number of moles of drug on the surface obtained at some high concentration of the drug in the contacting solution.

Table 2 shows values of the ion current, at --6.0 V, for a conical nanopore sensor at high concentrations of Hoechst 33258. We observed that the current decreases to a minimum and then increases again at concentrations above approximately 1 mM. This increase at high concentration results because the drug concentration is comparable to the electrolyte concentration, and the drug begins to contribute to the bulk conductivity of the electrolyte. Based on these results, we assume that $mole_{D,max}$ occurs for a solution drug concentration of 25 μM, and we call the current obtained I_{min}. If we call the (larger) current obtained in the absence of drug I_0, then $mole_{D,max}$ is proportional to the difference $I_0 - I_{min}$.

Likewise, if we call the current observed at some intermediate drug concentration, i, I_i then $mole_{D,i}$ is proportional to the difference $I_0 - I_i$. This allows us to calculate Θ for any concentration of drug, i, via:

$$\Theta_i = I_o - I_i/I_o - I_{min} \quad (3)$$

Equating these Θ values to the corresponding concentration values (Equation 1) allows us to plot out the Langmuir isotherm, and by fitting the experimental data to Equation 1, the value of the binding constant, K, can be obtained. Figure 4 shows the experimental and calculated plots, and a value of $K = 2 \times 10^5$ was obtained from the best fit. This K quantifies what the experimental data already taught us – Hoechst 33258 binds strongly to the Kapton surface.

Figure 4. Plot of surface coverage (Θ) versus concentration of the analyte drug Hoechst 33258.

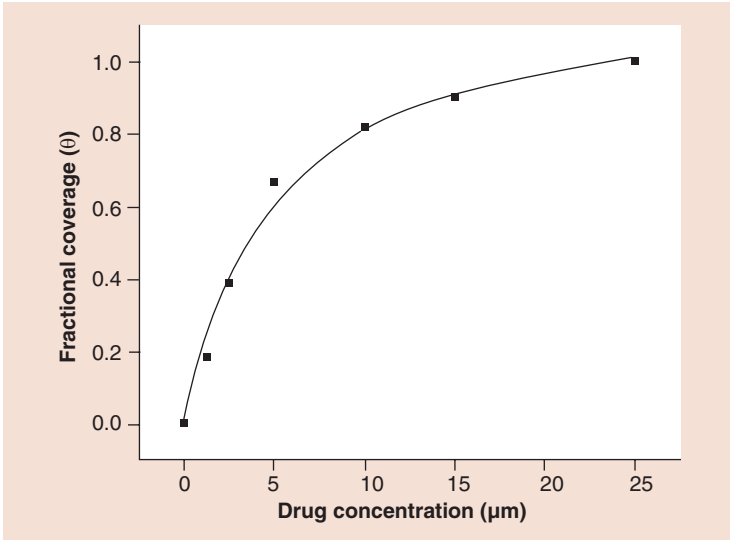

Points are experimental data; curve is best-fit calculation.

Conclusions

The sensor described here is reminiscent of much earlier work on ion-selective electrodes, potentiometric sensors, for hydrophobic drug molecules [55,56]. Both sensors use a hydrophobic membrane with fixed negative charge to extract hydrophobic cations into the membrane. In both cases, the sensor has greater selectivity for hydrophobic analytes relative to more hydrophilic analytes. In the case of the ion-selective electrode, this was quantified by investigating the response of the device to a homologous series of alkyl ammonium ions [56]. We are currently conducting studies of this type for the sensor described here.

The disadvantage of this hydrophobic-based selectivity paradigm is that the device cannot discriminate between analytes of similar mass and charge. In successful (commercially available) ion-selective electrodes, this problem is solved by incorporating a highly selective ionophore into the membrane. This could be accomplished with the sensor described here by simply attaching the ionophore to the pore walls. Finally, it is important to point out that with our current sensor design, the drug molecule binds not only to the pore walls but also to the faces of the membrane. This is because the pore walls and membrane faces are chemically identical. If adsorption to the membrane faces could be blocked, then a much smaller number of sites, only those along the pore walls, would be available for analyte adsorption. This would shift the isotherm to much lower analyte concentrations, and lower detection limits would be achieved. This could be accomplished by attaching a neutral and hydrophilic chemical species to the membrane faces.

Future perspective

Methods for improving both the selectivity and sensitivity of the sensor must be developed.

Acknowledgments

The authors would like to thank Henry Freiser for teaching them about the hydrophobic effect. We also acknowledge support from a State of Florida Center of Excellence Grant on Nano/Bio Sensors.

Financial and competing interests disclosure

The authors have no relevant affiliations or financial involvement with any organization or entity with a financial interest in or financial conflict with the subject matter or materials discussed in the manuscript. This includes employment, consultancies, honoraria, stock ownership or options, expert testimony, grants or patents received or pending, or royalties.

No writing assistance was utilized in the production of this manuscript.

Executive summary

Nanopore-based sensors

- There is increasing interest in using nanopores in synthetic or biological membranes as biosensors. A new nanopore-based sensing paradigm is described in this article.

Ion-current measurements & rectification

- This sensing paradigm entails placing an electrolyte solution on either side of the nanopore membrane, applying a transmembrane potential and measuring the resulting ion current flowing through the nanopore. If the small diameter (tip) opening of the nanopore is sufficiently small and if the nanopore has fixed surface charge, the nanopore will rectify the ion current.

Key results

- The fixed surface charge for these membranes is negative and the pore wall is hydrophobic. Exposure to a hydrophobic cationic drug causes the drug to adsorb to the pore wall, and this changes the extent rectification. In this way, the drug is sensed.

Bibliography

1. Martin CR, Bayley HC: Resistive-pulse sensing – from microbes to molecules. *Chem. Rev.* 100(7), 2575–2594 (2000).
2. Henriquez RR, Ito T, Sun L, Crooks RM: The resurgence of coulter counting for analyzing nanoscale objects. *Analyst* 129(6), 478–482 (2004).
3. Choi Y, Baker LA, Hillebrenner H, Martin CR: Biosensing with conically shaped nanopores and nanotubes. *Phys. Chem. Chem. Phys.* 8(43), 4976–4988 (2006).
4. Siwy ZS, Trofin L, Kohli P, Baker LA, Trautmann C, Martin CR: Protein biosensors based on biofunctionalized concial gold nanotubes. *J. Am. Chem. Soc.* 127(14), 5000–5001 (2005).
5. Park SR, Peng H, Ling XS: Fabrication of nanopores in silicon chips using feedback chemical etching. *Small* 3, 116–119 (2007).
6. Harrell CC, Choi Y, Horne LP, Baker LA, Siwy ZS, Martin CR: Resistive-pulse DNA detection with a conical nanopore sensor. *Langmuir* 22, 10837–10843 (2006).
7. Heins EA, Siwy ZS, Baker LA, Martin CR: Detecting single porphyrin molecules in a conically shaped synthetic nanopore. *Nano Lett.* 5, 1824–1829 (2005).
8. Saleh OA, Sohn LL: An artificial nanopore for molecular sensing. *Nano Lett.* 3, 37–38 (2003).
9. Saleh OA, Sohn LL: Direct detection of antibody–antigen binding using an on-chip artificial pore. *Proc. Natl Acad. Sci. USA* 100, 820–824 (2003).
10. Li J, Stein D, McMullan C, Branton D, Aziz MJ, Golovchenko JA: Ion-beam sculpting at nanometer length scales. *Nature* 412, 166–169 (2001).
11. Li J, Gershow M, Stein D, Brandin E, Golovchenko JA: DNA molecules and configurations in a solid-state nanopore microscope. *Nat. Mater.* 2, 611–615 (2003).
12. Fologea D, Gershow M, Ledden B, McNabb DS, Golovchenko JA, Li J: Detecting single stranded DNA with a solid state nanopore. *Nano Lett.* 5, 1905–1909 (2005).
13. Chen P, Mitsui T, Farmer DB, Golovchenko J, Gordon RG, Branton D: Atomic layer deposition to fine-tune the surface properties and diameters of fabricated nanopores. *Nano Lett.* 4, 1333–1337 (2004).
14. Chen P, Gu J, Brandin E, Kim YR, Wang Q, Branton D: Probing single DNA molecule transport using fabricated nanopores. *Nano Lett.* 4, 2293–2298 (2004).
15. Han A, Schurmann G, Mondin G *et al.*: Sensing protein molecules using nanofabricated pores. *Appl. Phys. Lett.* 88, 093901 (2006).
16. Storm AJ, Chen JH, Ling XS, Zandbergen HW, Dekker C: Fabrication of solid-state nanopores with single-nanometre precision. *Nat. Mater.* 2, 537–540 (2003).
17. Storm AJ, Chen JH, Zandbergen HW, Dekker C: Translocation of double-strand DNA through a silicon oxide nanopore. *Phys. Rev. E* 71, 051903 (2005).
18. Sun L, Crooks RM: Single carbon nanotube membranes: a well-defined model for studying mass transport through nanoporous materials. *J. Am. Chem. Soc.* 122, 12340–12345 (2000).
19. Uram JD, Ke K, Hunt AJ, Mayer M: Label-free affinity assays by rapid detection of immune complexes in submicrometer pores. *Angew. Chem. Int. Ed.* 45, 2281–2285 (2006).
20. Chang H, Kosari F, Andreadakis G, Alam MA, Vasmatzis G, Bashir R: DNA-mediated fluctuations in ionic current through silicon oxide nanopore channels. *Nano Lett.* 4, 1551–1556 (2004).
21. Smeets RM, Keyser UF, Krapf D, Wu MY, Dekker NH, Dekker C: Salt dependence of ion transport and DNA translocation through solid-state nanopores. *Nano Lett.* 6, 89–95 (2006).
22. Bayley H, Cremer PS: Stochastic sensors inspired by biology. *Nature* 1, 413, 226–230 (2001).
23. Gu LQ, Braha O, Conlan S, Cheley S, Bayley H: Stochastic sensing of organic analytes by a pore-forming protein containing a molecular adapter. *Nature* 398, 686–690 (1999).
24. Howorka S, Cheley S, Bayley H: Sequence-specific detection of individual DNA strands using engineered nanopores. *Nat. Biotechnol.* 19, 636–639 (2001).
25. Kasianowicz JJ, Burden DL, Han LC, Cheley S, Bayley H: Genetically engineered metal ion binding sites on the outside of a channel's transmembrane β-barrel. *Biophys. J.* 76, 837–845 (1999).
26. Braha O, Gu LQ, Zhou L, Lu X, Cheley S, Bayley H: Simultaneous stochastic sensing of divalent metal ions. *Nat. Biotechnol.* 18, 1005–1007 (2000).
27. Astier Y, Braha O, Bayley H: Toward single molecule DNA sequencing: direct identification of ribonucleoside and deoxyribonucleoside 5´-monophosphates by using an engineered protein nanopore equipped with a molecular adapter. *J. Am. Chem. Soc.* 128, 1705–1710 (2006).
28. Guan X, Gu LQ, Cheley S, Braha O, Bayley H: Stochastic sensing of TNT with a genetically engineered pore. *Chem. Biol. Chem.* 6, 1875–1881 (2005).
29. Howorka S, Nam J, Bayley H, Kahne D: Stochastic detection of monovalent and bivalent protein-ligand interactions. *Angew. Chem. Int. Ed.* 43, 842–846 (2004).
30. Movileanu L, Howorka S, Braha O, Bayley H: Detecting protein analytes that modulate transmembrane movement of a polymer chain within a single protein pore. *Nat. Biotechnol.* 18, 1091–1095 (2000).
31. Bezrukov SM, Vodyanoy I, Brutyan RA, Kasianowicz JJ: Dynamics and free energy of polymers partitioning into a nanoscale pore. *Macromolecules* 29, 8517–8522 (1996).
32. Henrickson SE, Misakian M, Robertson B, Kasianowicz JJ: Driven DNA transport into an asymmetric nanometer-scale pore. *Phys. Rev. Lett.* 85, 3057–3060 (2000).
33. Kasianowicz JJ, Henrickson SE, Weetall HH, Robertson B: Simultaneous multianalyte detection with a nanometer-scale pore. *Anal. Chem.* 73, 2268–2272 (2001).
34. Kasianowicz JJ, Brandin E, Branton D, Deamer DW: Characterization of individual polynucleotide molecules using a membrane channel. *Proc. Natl Acad. Sci. USA* 93, 13770–13773 (1996).
35. Meller A, Nivon L, Brandin E, Golovchenko J, Branton, D: Rapid nanopore discrimination between single polynucleotide molecules. *Proc. Natl Acad. Sci. USA* 97, 1079–1084 (2000).
36. Meller A, Nivon L, Branton D: Voltage-driven DNA translocations through a nanopore. *Phys. Rev. Lett.* 86, 3435–3438 (2001).
37. Meller A, Branton D: Single molecule measurements of DNA transport through a nanopore. *Electrophoresis* 23, 2583–2591 (2002).
38. Deamer DW, Branton D: Characterization of nucleic acids by nanopore analysis. *Acc. Chem. Res.* 35, 817–825 (2002).
39. Bezrukov SM, Kullman L, Winterhalter M: Probing sugar translocation through maltoporin at the single channel level. *FEBS Lett.* 476, 224–228 (2000).
40. Sexton LT, Horne LP, Sherrill SA, Bishop GW, Baker LA, Martin CR: Resistive-pulse studies of proteins and protein/antibody complexes using a conical nanotube sensor. *J. Am. Chem. Soc.* 129, 13144 – 13152 (2007).

41. Siwy Z, Heins E, Harrell CC, Kohli P, Martin CR: Conical nanotube ion-current rectifiers – the role of surface charge. *J. Am. Chem. Soc.* 126, 10850–10851 (2004).
42. Harrell CC, Kohli P, Siwy Z, Martin CR: DNA-nanotube artificial ion channels. *J. Am. Chem. Soc.* 126, 15646–15647 (2004).
43. Woermann D: Analysis of non-ohmic electrical current-voltage characteristic of membranes carrying a single track-etched conical pore. *Nucl. Instrum. Methods B* 194, 458–462 (2002).
44. Woermann D: Electrochemical transport properties of a cone-shaped nanopore: high and low electrical conductivity states depending on the sign of an applied electrical potential difference. *Phys. Chem. Chem. Phys.* 5, 1853–1858 (2003).
45. Woermann D: Electrochemical transport properties of a cone-shaped nanopore: Revisited. *Phys. Chem. Chem. Phys.* 6, 3130–3132 (2004).
46. Siwy ZS, Gu Y, Spohr HA *et al.*: Rectification and voltage gating of ion currents in a nanofabricated pore. *Europhys. Lett.* 60, 349–355 (2002).
47. Siwy ZS: Ion-current rectification in nanopores and nanotubes with broken symmetry. *Adv. Funct. Mater.* 16, 735–746 (2006).
48. Constantin D, Siwy ZS: Poisson–Nernst–Planck model of ion current rectification through a nanofluidic diode. *Physical Review E* 76, 041202 (2007).
49. Apel PY, Korchev YE, Swiy Z, Spohr R, Yoshida M: Diode-like single-ion track membrane prepared by electro-stopping. *Nucl. Instrum. Methods Phys. Res. Sect. B* 184, 337–346 (2001).
50. Wharton JE, Jin P, Sexton LT, Horne LP, Sherrill SA, Martin CR: A method for reproducibly preparing synthetic nanopores for resistive-pulse biosensors. *Small* 3(8), 1424–1430 (2007).
51. Siwy Z, Apel P, Dobrev D, Neumann RS, Trautmann C, Voss K: Ion transport through asymmetric nanopores prepared by ion track etching. *Nucl. Instrum. Methods Phys. Res. Sect. B* 208, 143–148 (2003).
52. Harrell CC, Siwy Z, Martin CR: Conical nanopore membranes – controlling the nanopore shape. *Small* 2, 194–198 (2006).
53. Teng M, Usman N, Frederick CA, Wang A: The molecular structure of the complex of Hoechst 33258 and the DNA didecaner d(CGCGAATTCGCG). *Nucleic Acids Res.* 16, 2671–2690 (1998).
54. Steinle ED, Mitchell DT, Wirtz M, Lee SB, Young VY, Martin CR: Ion-channel mimetic micropore and nanotube membrane sensors. *Anal. Chem.* 74, 2416–2422 (2002).
55. Martin CR, Freiser H: Ion-selective electrode for the determination of phencyclidine. *Anal. Chem.* 52, 1772–1774 (1980).
56. Martin CR, Freiser H: Response characteristics of ion selective electrodes based on dinonylnaphthalenesulfonic acid. *Anal. Chem.* 52, 562–564 (1980).